[44] Institut National de Physique Nucléaire et de Physique des Particules, 3 Rue Michel-Ange, 75794 Paris Cédex 16, France
[45] Institute for Astronomy, University of Edinburgh, Royal Observatory, Blackford Hill, Edinburgh EH9 3HJ, UK
[46] European Space Agency, ESRIN, Largo Galileo Galilei 1, 00044 Frascati, Roma, Italy
[47] Univ. Lyon, Univ. Claude Bernard Lyon 1, CNRS/IN2P3, IP2I Lyon, UMR 5822, 69622 Villeurbanne, France
[48] Observatoire de Sauverny, École Polytechnique Fédérale de Lausanne, 1290 Versoix, Switzerland
[49] Department of Astronomy, University of Geneva, Ch. d'Écogia 16, 1290 Versoix, Switzerland
[50] Department of Physics, Oxford University, Keble Road, Oxford OX1 3RH, UK
[51] Jodrell Bank Centre for Astrophysics, Department of Physics and Astronomy, University of Manchester, Oxford Road, Manchester M13 9PL, UK
[52] INFN-Padova, Via Marzolo 8, 35131 Padova, Italy
[53] Istituto Nazionale di Astrofisica (INAF) Osservatorio di Astrofisica e Scienza dello Spazio (OAS), Via Gobetti 93/3, 40127 Bologna, Italy
[54] Istituto Nazionale di Fisica Nucleare, Sezione di Bologna, Via Irnerio 46, 40126 Bologna, Italy
[55] INAF-Osservatorio Astronomico di Padova, Via dell'Osservatorio 5, 35122 Padova, Italy
[56] Max Planck Institute for Extraterrestrial Physics, Giessenbachstr. 1, 85748 Garching, Germany
[57] Universitäts-Sternwarte München, Fakultät für Physik, Ludwig-Maximilians-Universität München, Scheinerstrasse 1, 81679 München, Germany
[58] Institute of Theoretical Astrophysics, University of Oslo, PO Box 1029 Blindern, 0315 Oslo, Norway
[59] Jet Propulsion Laboratory, California Institute of Technology, 4800 Oak Grove Drive, Pasadena, CA 91109, USA
[60] von Hoerner & Sulger GmbH, Schloß-Platz 8, 68723 Schwetzingen, Germany
[61] Technical University of Denmark, Elektrovej 327, 2800 Kgs. Lyngby, Denmark
[62] Max-Planck-Institut für Astronomie, Königstuhl 17, 69117 Heidelberg, Germany
[63] Department of Physics and Helsinki Institute of Physics, University of Helsinki, Gustaf Hällströmin katu 2, 00014 Helsinki, Finland
[64] NOVA Optical Infrared Instrumentation Group at ASTRON, Oude Hoogeveensedijk 4, 7991 PD Dwingeloo, The Netherlands
[65] Argelander-Institut für Astronomie, Universität Bonn, Auf dem Hügel 71, 53121 Bonn, Germany
[66] Department of Physics, Institute for Computational Cosmology, Durham University, South Road, DH1 3LE, UK
[67] INFN-Bologna, Via Irnerio 46, 40126 Bologna, Italy
[68] Institute of Physics, Laboratory of Astrophysics, Ecole Polytechnique Fédérale de Lausanne (EPFL), Observatoire de Sauverny, 1290 Versoix, Switzerland
[69] European Space Agency, ESTEC, Keplerlaan 1, 2201 AZ Noordwijk, The Netherlands
[70] Department of Physics and Astronomy, University of Aarhus, Ny Munkegade 120, 8000 Aarhus C, Denmark
[71] Space Science Data Center, Italian Space Agency, Via del Politecnico snc, 00133 Roma, Italy
[72] Institute of Space Science, Bucharest 077125, Romania
[73] Instituto de Astrofísica de Canarias, Calle Vía Láctea, s/n, 38204 San Cristóbal de La Laguna, Tenerife, Spain
[74] Departamento de Astrofísica, Universidad de La Laguna, 38206 La Laguna, Tenerife, Spain
[75] Aix-Marseille Univ., CNRS/IN2P3, CPPM, Marseille, France
[76] Dipartimento di Fisica e Astronomia "G. Galilei", Università di Padova, Via Marzolo 8, 35131 Padova, Italy
[77] Aix-Marseille Univ., CNRS, CNES, LAM, Marseille, France
[78] Centro de Investigaciones Energéticas, Medioambientales y Tecnológicas (CIEMAT), Avenida Complutense 40, 28040 Madrid, Spain
[79] Instituto de Astrofísica e Ciências do Espaço, Faculdade de Ciências, Universidade de Lisboa, Tapada da Ajuda, 1349-018 Lisboa, Portugal
[80] Universidad Politécnica de Cartagena, Departamento de Electrónica y Tecnología de Computadoras, 30202 Cartagena, Spain
[81] Kapteyn Astronomical Institute, University of Groningen, PO Box 800, 9700 AV Groningen, The Netherlands
[82] Infrared Processing and Analysis Center, California Institute of Technology, Pasadena, CA 91125, USA
[83] INAF-Osservatorio Astronomico di Brera, Via Brera 28, 20122 Milano, Italy
[84] Institut d'Astrophysique de Paris, UMR 7095, CNRS, et Sorbonne Université, 98 bis Boulevard Arago, 75014 Paris, France
[85] Junia, EPA Department, 59000 Lille, France

Appendix A: The curvature pro le

The analyses presented in this paper rely on the assumption of the compensated pro le introduced in Sect. 2.2, which was chosen in order to ensure that the CDM background is recovered at r r_B, a crucial feature in order to confront CMB data consistently using an ective FLRW model.

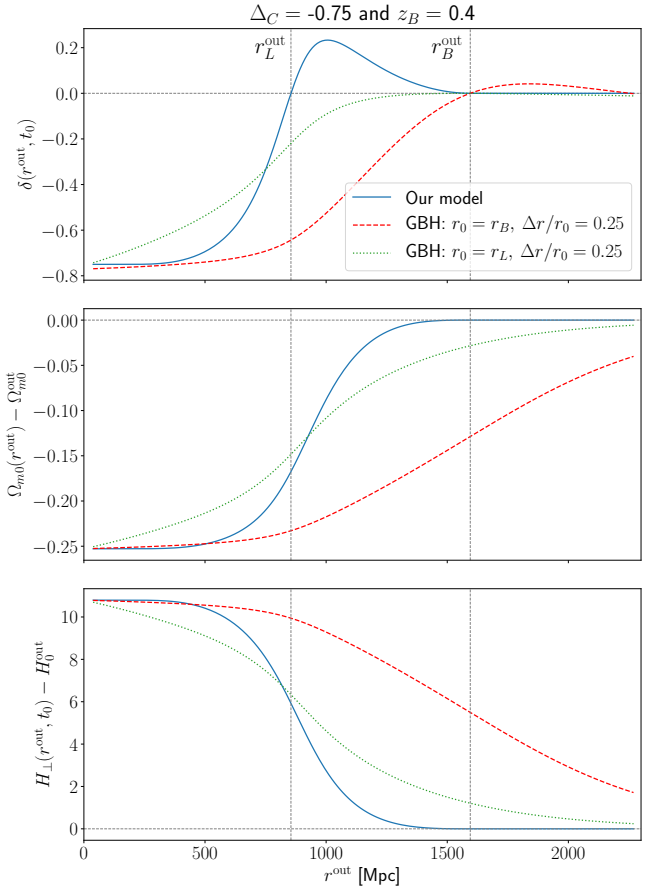

Fig. A.1. Comparison between our model and the GBH parametrization. Top: Density contrast of matter today (r; t_0), as a function of the FLRW comoving coordinate. Our compensated model (solid blue line) satis es (r_L^out; t_0) = (r_B^out; t_0) = 0, while the CDM background is not exactly recovered for the GBH models (dashed red and dotted green lines). Middle: Deviations from the background density of matter, _m;0^out, as a function of the FLRW comoving coordinate. The GBH model with r_0 = r_B (red dashed line) largely deviates from _m;0^out at r^out = r_B^out. On the other hand, the choice of = r_L for the GBH leads to deviations of approximately 0:01 from the background at r^out = r_B^out. The model assumed in this work fully recovers _m;0^out at any r^out r_B^out. Bottom: Deviations from the background Hubble expansion as a function of the FLRW comoving coordinate. GBH models (dashed red and dotted green lines) do not perfectly match the CDM background expansion history at r^out = r_B^out.

Here, we compare our model to the Garcia-Bellido and Haugboelle (GBH) model (Garcia-Bellido & Haugboelle 2008a), which parametrises the LTB metric by imposing

$$ {}_{m;0}(r) = {}_{m;0}^{\rm out} + \left({}_{m;0}^{\rm in} - {}_{m;0}^{\rm out}\right)\left(\frac{1 - \tanh[(r - r_0)/2\ r]}{1 + \tanh[r_0/2\ r]}\right); $$

$$ H_0(r) = H_{?0}^{\rm out} + \left(H_{?0}^{\rm in} - H_{?0}^{\rm out}\right)\left(\frac{1 - \tanh[(r - r_0)/2\ r]}{1 + \tanh[r_0/2\ r]}\right); $$

where r_0 is the size of the void, r the transition scale, _m;0^in _m;0(r = 0), and H_?0^in H_?0(r = 0). Fig. A.1 shows the differences between our model (solid blue line) and the GBH model, where we have adopted r_0 = r_L (dotted green line) and r_0 = r_B (dashed red line). When the size of the GBH inhomogeneity is xed to r_B, a scale greater than r_B is needed to recover the CDM background. On the other hand, if one assumes r_0 = r_L, the GBH model tends to the CDM background at r = r_B. In contrast, our model perfectly matches the CDM background at any scale r_B. The compensating behaviour of our model is particularly notable in the top panel of the Fig. A.1, where we note that (r_L^out; t_0) = (r_B^out; t_0) = 0 for our model while the GBH models does not satisfy (r^out; t_0) = 0 for all r^out r_B^out.

Furthermore, to investigate the dependence of our results on the chosen pro le, we performed an additional analysis using the following generalisation of Eq. (10):

$$ P_3(x;) = \begin{cases} 1 & \text{for } 0 \quad x < \\ 1 \quad \exp\left[\frac{1}{x}(1 - \frac{x}{1})^3\right] & \text{for } \quad x < 1\ ; \\ 0 & \text{for } 1 \quad x \end{cases} \qquad \text{(A.1)} $$

with 0 < < 1. This new parameter will modify the smoothness of the transition between the inner and compensating region, leading to sharpened pro les when approximates to 1. Results from this extra analysis, which is performed using the combination Base + BAO + Euclid + DESI + y-dist. + kSZ from the CDM ducial, shows that the inclusion of the parameter weakens the constraints on _c and r_L^out by a factor of two, compared to the results from Eq. (10).

Appendix B: Re-scaling datasets

Covariance matrices are fundamental pieces of forecast analyses. However, their production for forthcoming surveys is an open issue when non-standard cosmologies are considered (Harnois-Deraps et al. 2019; Friedrich et al. 2021; Ferreira & Marra 2022). This complicates the construction of forecast data for LTB cosmologies. Nesseris et al. (2022) has overcome this issue by neglecting the error due to the non-standard cosmology. Here, we apply a re-scaling method to convert the CDM forecast data and its covariance matrices into LTB catalogues.

Consider a given dataset, with x_i being the observed quantity, z_i the corresponding redshift, and C_ij the covariance matrix. This dataset can be re-scaled to agree with a particular model via the following steps.

First, we de ne R_ij = C_ij / x_i x_j, a new matrix that contains the relative uncertainties and correlations from the original covariance matrix. Second, we compute with the theoretical prediction of the new model the ducial values at the relevant redshifts, such that x_i^f x^d(z_i). Third, using the above de ned quantities, we compute the new correlation matrix C_ij = x_i^f x_j^f R_ij. Finally, we then draw a random realisation, x_i, of the multivariate-normal distribution N(x_i^f; C_ij).

We note that this method assumes that relative error and correlations are not changed by a non-standard model. As discussed through this paper, the procedure above is also applied to re-scale real data according the ducial models presented on Table 1; this ensures that all data are consistently described by a particular ducial model.

Appendix C: The inhomogeneous Hubble constant

The LTB model features a pro le function $H_0(r)$ that depends on the radial distance from the centre of the void, instead of a constant value like H_0 in the ΛCDM model. Since there is not a preferable scale to set the rate of expansion of the Universe, the de nition of H_0 remains arbitrary. To overcome this issue, we extend the FLRW de nitions and mimic the observational procedure to locally constrain the Hubble constant. Explicitly, we adopt the de nition H_0^L for inhomogeneous cosmological models that was introduced in Camarena et al. (2022). This method, which is applied for every sample point of the parameter space, follows the following steps.

First, we create a mock catalogue using the redshifts of Pantheon SNe at $0.023 < z < 0.15$ and the LTB luminosity distances at the corresponding redshifts. Second, the mock data are tted using an extension of the cosmographic expansion given by

$$D_L(z) = \frac{cz}{H_0^L}\left[1 + \frac{(1 - q_0^r)z}{2}\right]; \tag{C.1}$$

$$q_0^r(r) = \frac{\Omega_m(r)}{2} - \Omega_\Lambda(r)\left[\frac{H_0(r)}{H_0^L}\right]^2; \tag{C.2}$$

where q_0^r is the radial-dependent deceleration parameter. Finally, the best- t value of H_0^L is adopted as the measured Hubble constant.

It is interesting to point out that this procedure mimics the standard cosmic distance ladder analysis of SNe that follow the Hubble ow, while taking into account the e ect of the inhomogeneity on the measurement of the Hubble constant. We note that other authors have previously proposed similar approximations (Redlich et al. 2014; Efstathiou 2021).